Available online at www.sciencedirect.com
ScienceDirect
European Journal of Pharmaceutics and Biopharmaceutics 66 (2007) 334–347
European Journal of Pharmaceutics and Biopharmaceutics
www.elsevier.com/locate/ejpb

Research paper

Investigation of the release mechanism of a sparingly water-soluble drug from solid dispersions in hydrophilic carriers based on physical state of drug, particle size distribution and drug–polymer interactions

Evangelos Karavas [a,b], Emmanuel Georgarakis [b], Michael P. Sigalas [c], Konstantinos Avgoustakis [d], Dimitrios Bikiaris [e,*]

[a] *Pharmathen S.A., Pharmaceutical Industry, Attiki, Greece*
[b] *Department of Pharmacy, Aristotle University of Thessaloniki, Thessaloniki, Greece*
[c] *Department of Chemistry, Aristotle University of Thessaloniki, Thessaloniki, Greece*
[d] *Department of Pharmacy, University of Patras, Patras, Greece*
[e] *Department of Chemistry, Aristotle University of Thessaloniki, Thessaloniki, Greece*

Received 13 September 2006; accepted in revised form 23 November 2006
Available online 1 December 2006

Abstract

In the present study the release mechanism of the sparingly water-soluble drug felodipine (FELO) from particulate solid dispersions in PVP or PEG was investigated. FT-IR data indicated that a N–H···O hydrogen bond is formed between FELO and polymers. The drug–polymer interaction was theoretically studied with the density functional theory with the B3LYP exchange correlation function. The interaction energies have been estimated at −31.8 kJ/mol for PVP and −18.8 kJ/mol for PEG. Also, detailed vibrational analysis of the complexes showed that the red shift of the N–H bond stretching in FELO molecule due to H-bonding was higher in the FELO–PVP complex than in the FELO–PEG complex. Both the experimental and theoretical data indicated that a stronger interaction of FELO with PVP than with PEG was developed. The interactions of FELO with the polymer appeared to control the physical state (amorphous or crystalline) and the particle size of FELO in the solid dispersions. In the FELO/PVP dispersions, the drug is found as amorphous nanoparticles whereas in FELO/PEG dispersions the drug is dispersed as crystalline microparticles. The size of drug particles in the dispersion was also influenced by drug proportion, with an increase in drug content of the dispersion resulting in increased drug particle size. The particle size of drug, the proportion of drug in the dispersion and the properties of the polymer (molecular weight) appeared to determine the mechanism of drug release from the solid dispersions, which was drug diffusion (through the polymer layer)-controlled at low drug contents and drug dissolution-controlled at high drug contents. In situ DLS measurements indicate that the large initial particles of FELO/PVP and FELO/PEG solid dispersions with low drug content (10–20 wt%) are very rapidly decreased to smaller particles (including nanoparticles) during dissolution, leading to the observed impressive enhancement of FELO release rate from these dispersions.

Keywords: Felodipine; PVP; PEG; Solid dispersion; Sparingly soluble drugs; Dissolution enhancement

1. Introduction

The enhancement of the bioavailability of poorly water-soluble drugs is one of the greatest challenges of drug development and several pharmaceutical technologies have been investigated to this end. Amongst them is the dispersion of the drug into an inert, hydrophilic polymer matrix

* Corresponding author. Laboratory of Organic Chemical Technology, Department of Chemistry, Aristotle University of Thessaloniki, 541 24 Thessaloniki, Greece. Tel.: +30 2310 997812; fax: +30 2310 997769.
E-mail address: dbic@chem.auth.gr (D. Bikiaris).

0939-6411/$ - see front matter © 2006 Elsevier B.V. All rights reserved.
doi:10.1016/j.ejpb.2006.11.020

[1,2]. Although a large number of studies have been published on the subject, the mechanisms underpinning the observed enhancement of the rate of drug release are not yet understood [3,4]. The reason for this lies in the complexity of the release process and the multitude of factors that can affect it, including the properties of drug (solubility [5], physical state [6], particle size [7]), the properties of the polymer forming the matrix (dissolution rate [8], molecular weight [9] and the possible drug–polymer interaction [10,11]). Craig proposed a simplified drug release model differentiating between carrier-controlled and drug-controlled dissolution, depending on drug solubility in the concentrated polymer layer that is formed on the dissolving surface [3]. The proposed model might help to identify the correct strategy to control (improve) the release rate of drug from the solid dispersion (the strategy will depend on release mechanism, i.e. if the release is carrier- or drug-controlled) and perhaps most importantly to understand the causes of possible formulation instability upon storage and select scientifically sound approaches to deal with it. Although useful as methodological approach in identifying possible dominant mechanisms of drug release from solid dispersions, the model is based on several assumptions that may not hold in many cases. For example, drug release by diffusion through the polymer layer is considered to be too slow to exert any significant effect on drug release. However, this may not be true especially in the case of low molecular weight polymers.

Our long-term aim is to develop an immediate-release formulation of felodipine (FELO), which could be useful as an emergency treatment in ischemic heart disease. In our previous work, we have shown that the interaction (hydrogen bonding) between PVP and FELO affected drug solubility and particle size distribution of drug in the polymer matrix and that through these effects drug–polymer interaction affected drug release [12]. In this report, we provide evidence that felodipine release from solid dispersions in PVP or PEG is significantly enhanced due to a rapid dissolution of initial particles of the dispersion into smaller particles, including nanoparticles, and that the release mechanism changes gradually from a diffusion-controlled to a dissolution-controlled one with increasing drug proportion in the solid dispersion. The felodipine–polymer interactions at the molecular level have been evaluated, based on experimental ^{1}H NMR data (in solution), FT-IR data (in solid state) and theoretical quantum mechanical calculations, and their consequences with regard to the physical state of the drug in the dispersions and the drug release are discussed.

2. Experimental

2.1. Materials

Felodipine (FELO) with an assay of 99.9% was obtained from PCAS (Longjumeau, France) with a melting point of 143–145 °C and solubility in water approximately 0.5 mg/L while it is freely soluble in ethanol. Poly(vinyl pyrrolidone) (PVP) type Kollidon K30 with a molecular weight M_w of 50,000–55,000 was obtained from BASF (Ludwigshafen, Germany), $T_g = 167$ °C (DSC), moisture content 1.95% (TGA) and bulk density 0.410 g/cm^3. Poly(ethylene glycol) (PEG 4000) with a molecular weight of 3898 g/mol (calculated by OH end groups), $T_m = 54$ °C (DSC analysis), moisture content <0.5% (TGA analysis) and viscosity at 20 °C and 50% RH 118 mPa was obtained from CLARIANT (Germany). All other materials and reagents were of analytical grade of purity.

2.2. Preparation of felodipine nanodispersions in PVP and PEG matrices

Solid dispersions containing 10, 20, 30 and 50 wt% felodipine were prepared using PVP and PEG as drug carriers and 1 wt% sodium docusate. Sodium docusate was added to prevent drug particle aggregation during solvent evaporation. Accurately weighed quantities of the drug and the polymer were separately dissolved in absolute ethanol and after solubilization, the solutions were mixed and sonicated for 15 min. In order to evaporate the ethanol, the solutions were maintained at 40 °C for 48 h. The prepared films were pulverized and milled to a particle size of 109–250 μm. PEG films were cooled in liquid nitrogen prior to milling. The granules were assayed spectrophotometrically (UV–VIS) for FELO content at 362 nm by using a Shimadzu UV 1601 apparatus.

2.3. In vitro release profile [13]

The release rate of FELO from the granules was measured in a dissolution apparatus type DISTEK 2100B, equipped with an autosampler using the paddle method (USP II method). In each dissolution vessel quantities of solid dispersions equivalent to 10 mg FELO were placed. The test was performed at 37 ± 1 °C with a rotation speed of 100 rpm. The dissolution medium was 500 ml of 0.1 M phosphate buffer, pH 6.5, containing 2% Polysorbate 20. At predetermined time intervals, samples of 5 ml were withdrawn from the dissolution medium, filtered through 0.2 μm membranes and assayed spectrophotometrically for the drug at 362 nm. An equal volume of fresh dissolution medium was transferred to the flask after sample withdrawal.

2.4. X-ray diffraction (XRD)

XRD analysis of dispersions in the form of thin films was performed on randomly oriented samples, scanning over the interval 5–55° 2θ, in a Philips PW1710 diffractometer, with Bragg–Brentano geometry (θ, 2θ) and Ni-filtered CuKα radiation.

2.5. FT infrared spectroscopy

FT-IR spectra of the solid dispersions, formulated in KBr tablets containing 1 wt% of the sample, were obtained with a Perkin-Elmer FT-IR spectrometer (Spectrum 1000,

USA). The IR spectra, in absorbance mode, were obtained in the spectral region 450–4000 cm^{-1} using a resolution of 2 cm^{-1} and 64 co-added scans.

2.6. Scanning electron microscopy (SEM)

The morphology of the raw materials and solid dispersions was examined using a scanning electron microscope (SEM) type Jeol (JMS-840, Japan). The films were covered with a carbon coating in order to have good conductivity of the electron beam, under the following operating conditions: accelerating voltage 20 kV, probe current 45 nA and counting time 60 s.

2.7. Transmission electron microscopy (TEM)

Electron diffraction (ED) and Transmission electron microscopy (TEM) investigations were made on ultra-thin film samples of solid dispersions prepared by ultra-microtome operated with liquid nitrogen. The thin films were deposited on copper grids. TEM micrographs were obtained by using JEOL 120 CX microscope (Japan), operating at 120 kV. To avoid the destruction of PVP films by the electron radiation, the films were coated with carbon black before introducing them in the sample chamber of the microscope.

2.8. Quantum mechanical modeling of drug–polymer interactions

Density functional theory (DFT) full geometry optimizations of the studied molecules and the H-bonded complexes have been carried out using the Gaussian 98 suite of programs [14]. The basis set used was 6-31G. In order to achieve a better description of the hydrogen bond, the basis set for the atoms of the groups involved, that is (>NH) of felodipine, >C═O of PVP model and (—O—) of PEG model, has been augmented to 6-31G++(d,p). Harmonic frequency calculations were performed for all the optimized structures to establish that the stationary points found are minima. In calculating the interaction energy in the hydrogen-bonded complexes, we accounted for the basis set superposition error (BSSE) by recalculating the monomer energies using the full dimer basis at the optimized geometry of the dimer using the counterpoise method [15].

2.9. ^1H NMR spectroscopy

^1H NMR spectra of pure compounds and all prepared solid dispersions (containing 10/90, 20/80, 30/70 and 50/50 w/w FELO/PVP or FELO/PEG) were recorded in a BRUCKER DRX 400 MHz spectrometer. Deuteronized chloroform $CDCl_3$ was used as solvent.

2.10. Particle size analysis during dissolution

The particle size distribution of the FELO/PVP and FELO/PEG solid dispersions during dissolution was determined by dynamic light scattering (DLS) using a Zetasizer Nano Instrument (Malvern Instruments, Nano ZS, ZEN3600, UK) operating with a 532 nm laser. A suitable amount of solid dispersion was transferred to the dissolution medium (which was the same as the one used in the determination of the in vitro release profiles) creating a total concentration 1‰. The dissolution medium was kept at 37 °C and agitated at 100 rpm. Particle size was measured at different times after sample introduction into the dissolution medium.

3. Results

3.1. Release profiles

As it can be seen in Fig. 1 an impressive enhancement of FELO dissolution rate is achieved with both types of dispersion (FELO/PVP and FELO/PEG) containing 10 or 20 wt% FELO. Drug release is almost complete after 30 min from the 10 wt% dispersions and after 60 min from the 20 wt% dispersions. As the drug content of the dispersion increased, the rate of release became lower for both types of dispersion. The FELO/PEG dispersions exhibited a little lower release rates compared to the FELO/PVP dispersions of same drug content, the difference in release rate increasing with increasing drug content of the dispersions.

In order to investigate the mechanism of drug release, the release data were fitted (STATGRAPHICS Plus 4.0 software) to the two-term equation, which is used to describe drug release from polymer matrices taking place by a combination of drug diffusion and polymer dissolution (erosion) [16]:

$$Q = k_1(t)^{0.5} + k_2(t) \quad (1)$$

where Q is the % release at time t, and k_1, k_2 are the release constants for diffusion and dissolution, respectively.

It appears that with both types of dispersion there is a gradual switch from a diffusion-controlled to a dissolution-controlled drug release with increasing drug proportion in the dispersion (Table 1).

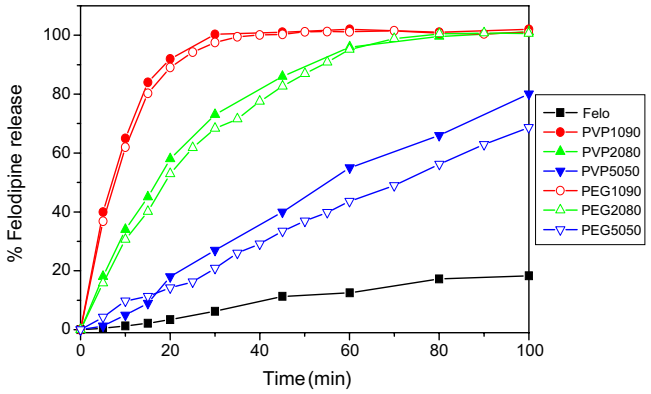

Fig. 1. Dissolution profiles of FELO/PVP and FELO/PEG solid dispersions containing different drug/polymer proportions. The dissolution profile of FELO alone is presented for comparison.

Table 1
Results from fitting felodipine release data (in the range 10–80% release) in equation: $Q = k_1(t)^{0.5} + k_2(t)$

Dispersion	k_1	k_2	R^2	% release by diffusion	% release by dissolution	Dissolution/diffusion
FELO/PVP 10/90 w/w	17.295	0.877	0.9916	80.846	19.162	0.237
FELO/PVP 20/80 w/w	9.197	0.622	0.9672	66.987	33.013	0.493
FELO/PVP 50/50 w/w	0.666	0.757	0.9847	7.365	92.589	12.571
FELO/PEG 10/90 w/w	15.279	1.175	0.9913	73.098	26.891	0.368
FELO/PEG 20/80 w/w	7.843	0.733	0.9769	58.795	41.210	0.701
FELO/PEG 50/50 w/w	0.596	0.631	0.9978	7.226	92.818	12.845

3.2. Physical characterization of solid dispersions

XRD diffraction patterns of FELO and its FELO/PVP-FELO/PEG solid dispersions revealed that FELO is a crystalline compound, showing a very strong diffraction peak at 2θ of 23.38° while others present a lower intense one at 2θ of 10.32°, 11.0°, 16.32°, 16.64°, 20.6°, 22°, 24.6°, 25.5° and 26.6° (Fig. 2a). However, even though it is a crystalline material, its dispersions in the PVP matrix are completely amorphous. Only two broad peaks that correspond to the diffraction pattern of pure PVP are recorded, while peaks that correspond to FELO crystals completely disappear, suggesting that the PVP matrix inhibits the crystallization of FELO (Fig. 2a) [17,18]. On the other hand FELO/PEG XRD diffraction patterns reveal that FELO recrystallizes during preparation of solid dispersions after solvent evaporation. PEG has two characteristic strong peaks at $2\theta = 19.9°$ and 23.35°. The same peaks are also recorded in all solid dispersions while the characteristic peak of FELO, particularly at 10.32°, can be distinguished, confirming that FELO is dispersed in a crystalline state within PEG. This behaviour is usually the case when PEG is used as the dispersion matrix, which as a semi-crystalline polymer assists drug crystallization.

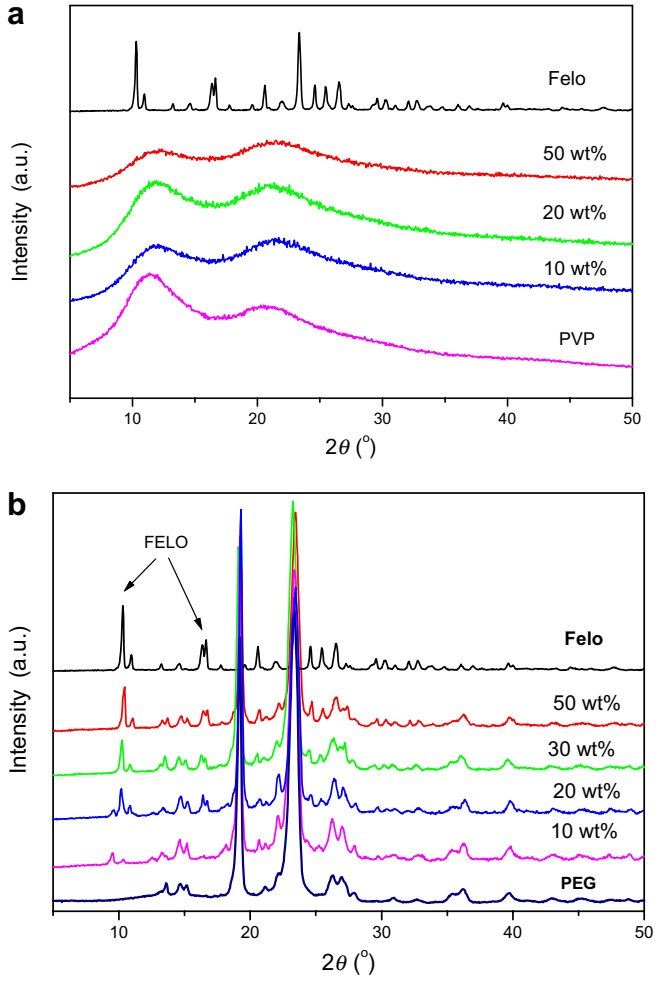

Fig. 2. XRD patterns of (a) FELO and FELO/PVP solid dispersions and (b) FELO and FELO/PEG solid dispersions.

In order to characterize the particle size distribution of felodipine in the PVP matrix, TEM was used since SEM, due to the drug's amorphization, is not sufficiently informative at a very small particle size range.

The size of the drug particles (black spots) was directly affected by drug proportion in the PVP matrix (Fig. 3). In FELO/PVP solid dispersion consisting of 90/10 w/w, particle sizes in the range of 20–130 nm were detected. By increasing the FELO content, the particle sizes gradually became larger, ranging within 50–200 and 500–1000 nm in solid dispersions, containing 20 and 50 wt% of FELO, respectively. In all cases, it is noticeable that these nanoparticles are not individual particles, but aggregates from individual particles having sizes of approx. 5–10 nm. Particles with high specific surface tent to aggregate; this trend is higher when increasing the drug concentration in the solid dispersion. In the case of FELO/PEG solid dispersions, the identification of FELO particles is relatively easy and thus SEM was used for their detection. Even in the dispersion systems containing relatively small drug amount, drug crystals can be easily distinguished in the polymer matrix (Fig. 4).

In the 10 wt% FELO/PEG dispersions, these crystals have the form of needles with a thickness that varies between 100 and 200 nm and with a length of 2–7 μm. In dispersions with higher FELO content, well-formed crystals with bigger sizes (with regard to their width) can be distinguished. These ranged within 0.3–1.1, 0.7–2.8 and 2–10 μm for the dispersions containing 10, 20 and 50 wt% FELO, respectively. The differentiation between the two crystal forms is probable due to the lower amount of felodipine in the case of FELO/PEG 10/90 w/w solid dispersion, at which more drug amount is in amorphous form

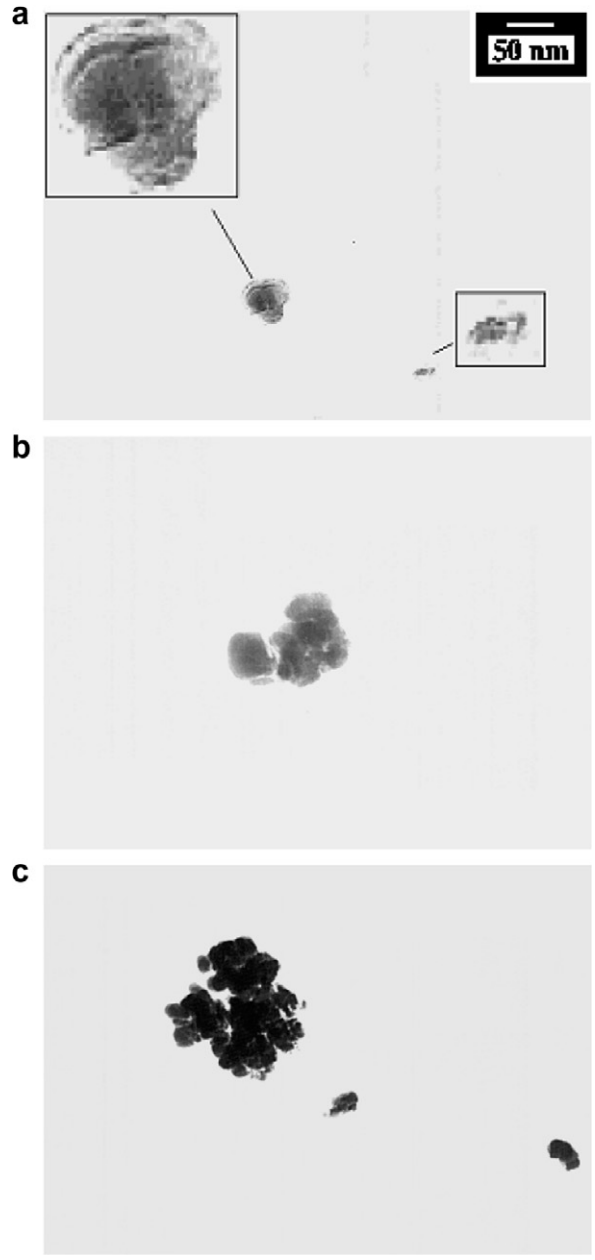

Fig. 3. Transmission electron photomicrographs of FELO/PVP nanodispersions containing different drug amounts: (a) 10/90 w/w (40–50 nm), (b) 20/80 w/w (100–110 nm) and (c) 50/50 w/w (500–550 nm).

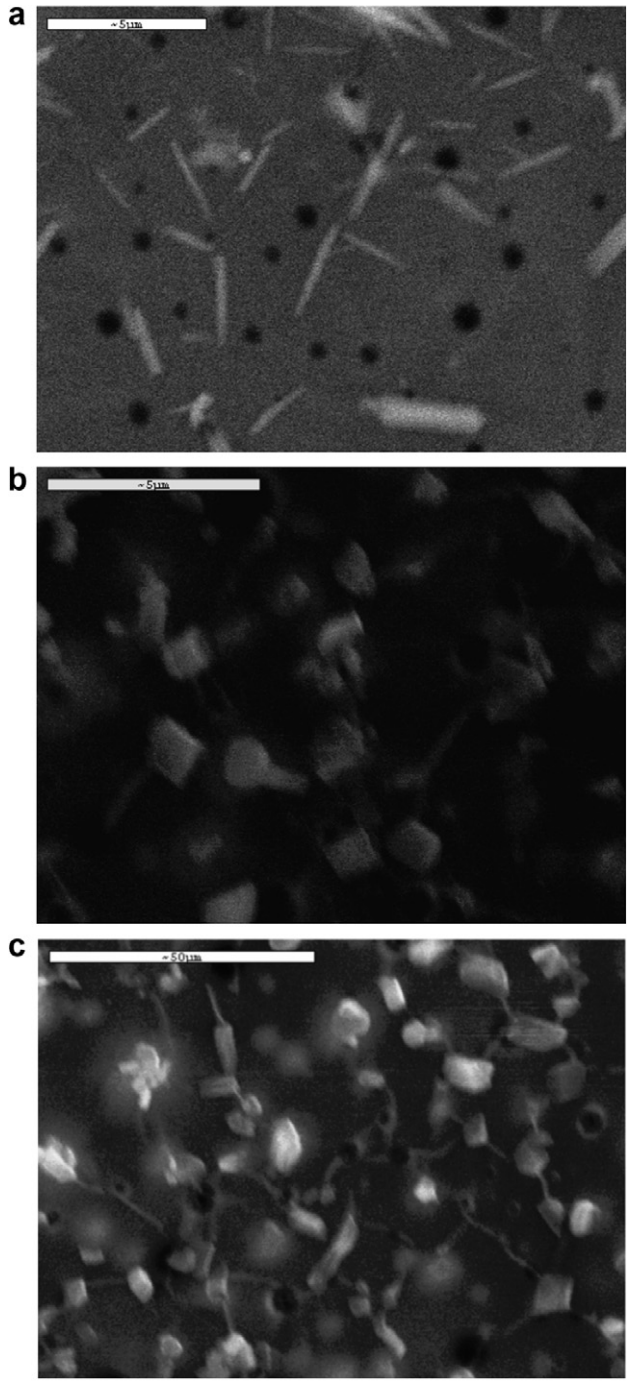

Fig. 4. SEM microphotographs of FELO/PEG solid dispersions: (a) 10/90 w/w, (b) 20/80 w/w and (c) 50/50 w/w.

and thus crystals in the form of needles are formed. As the drug amount increases the saturation of the solid dispersion becomes higher and thus the formed crystals have the same shape as that of neat drug.

3.3. Evaluation of the influence of drug–polymer interactions on physical state and particle size of felodipine

From the XRD and microscopy data, it became evident that not only the physical state but the particle size of the drug too is different in the two different dispersion types (FELO/PVP and FELO/PEG). To evaluate the degree at which this is due to the nature of the polymer (amorphous or crystalline) or the strength of the interactions between the reactive groups of drug and polymer molecules, FT-IR spectroscopy was used in conjunction with quantum mechanical calculations of interactions. It has been reported that interactions between the drug and polymer during solid dispersion preparation, and their extent, are responsible for the formation of amorphous or crystalline dispersions and possibly for the particle size distribution of the drug into the polymer matrix [10,11]. The FT-IR spectra

of FELO/PVP and FELO/PEG dispersions indicate that hydrogen bonds between the secondary amino-groups of FELO and the carbonyl groups of PVP or the backbone oxygen atoms and the chain end hydroxyl groups of PEG are formed (Fig. 5).

Specifically, in pure FELO the peak corresponding to the bond of its amino-group was recorded at 3370 cm^{-1}. In PVP solid dispersions this peak shifted towards lower wavenumbers. The exact position and its form depended on the FELO/PVP ratio (Fig. 5a). Thus, in dispersions containing 10 wt% FELO two peaks are recorded at 3292 and 3222 cm^{-1} indicating the existence of two kinds of hydrogen bonds: one kind concerns very strong hydrogen bonds and is recorded at the lower position and the other kind concerns hydrogen bonds of lower intensity recorded at the higher position. In dispersions with 20 or 50 wt% FELO, only one peak at 3292 and 3290 cm^{-1}, respectively, can be seen in the spectra, indicating that only weak hydrogen bonds are formed. This is in accordance with our previous study where it was found that, as FELO amount in the dispersion increased, the interactions became weaker, since, due to the bulkiness of the FELO molecule, each one molecule corresponds to four repeating units of PVP [12]. The low peak intensities corresponding to FELO are due to the broad and more intense peak of PVP at this area and due to the lower amount of drug in solid dispersions. The above-discussed wavelength range is the most characteristic for the evaluation of interactions concerning hydrogen bonding, since the absorbance of the carbonyl group of PVP in 1662 cm^{-1} is masked by the absorbance of FELO ester groups in the same area.

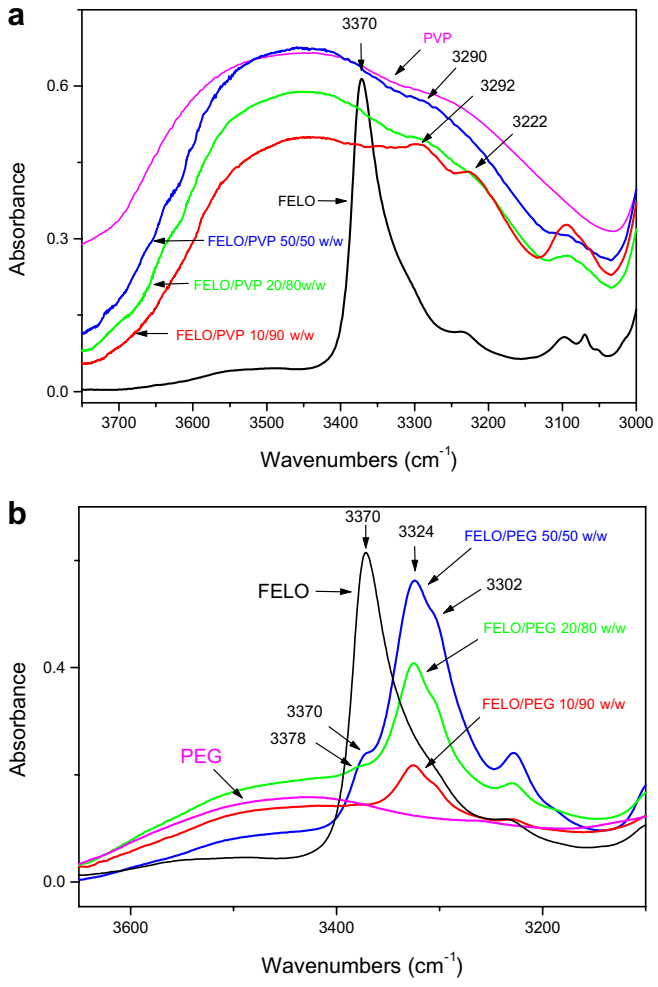

Fig. 5. FT-IR spectra of FELO/PVP (a) and FELO/PEG (b) solid dispersions.

In FELO/PEG solid dispersions similar shifts of secondary amino-groups of FELO in lower positions were also recorded (Fig. 5b). In all FELO/PEG dispersions, there is a strong peak recorded at 3324 cm^{-1} and some others of lower intensity at 3370 cm^{-1}. The latter is at the same position as in pure FELO, which is an indication that some FELO molecules did not interact with the —OH end groups or the —O— backbone groups of PEG. However, the main peak at 3324 cm^{-1} indicates that a certain degree of interaction between drug and PEG does occur. The neat shift of the secondary amino-group absorbance is in the case of PEG solid dispersions 46 cm^{-1} whereas in the case of PVP dispersions it is almost double, i.e. 80 cm^{-1}, indicating that these H-bonding interactions are more potent in the case of FELO/PVP dispersions.

In order to confirm that the drug/polymer interactions are more potent in the case of FELO/PVP dispersions, we advanced the estimate of these interactions with the growth of α quantum mechanical model, so as to theoretically evaluate this possibility [19–21]. The present reliability of high precision quantum mechanical calculations gives us the possibility to derive meaningful predictions about these weak interactions. The drawback of this is the need to restrict our consideration to a relatively small system representative of the whole polymer in vacuum. Thus, we used two low molecular weight models corresponding to the monomer units of PVP and PEG polymers, PVPm and PEGm, respectively (Fig. 6).

Their calculated global minimum energy structures are shown in Fig. 6. The $C_7{=}O_3$ bond length in PVPm is equal to 1.227 Å and for $C_{7,8}{-}O_3$ bonds in PEGm it is equal to 1.442 Å. The Mulliken charges for oxygen atoms, serving as intermolecular hydrogen bond acceptors, are −0.538 for PVPm and −0.685 for PEGm. The charges of the carbonyl oxygen atoms of felodipine being potential candidates for intermolecular hydrogen bonding with the $>N_1{-}H_1$ are equal to −0.465 and −0.530. Thus, in principle the intermolecular felodipine–polymer hydrogen bond should be stronger. Nevertheless, the intermolecular hydrogen bonds should also be disfavored for steric reasons. The optimized structure of the most stable conformer of felodipine (**1**) and the equilibrium geometries of the 1-PVPm and 1-PEGm complexes are shown in Fig. 6, while relevant optimized geometrical parameters involving the intermolecular hydrogen bonds that are responsible for the felodipine–polymer complex are given in Table 2. The complexes of felodipine, 1, and the polymer models PVPm and PEGm have been fully optimized at the B3LYP/6-31G level.

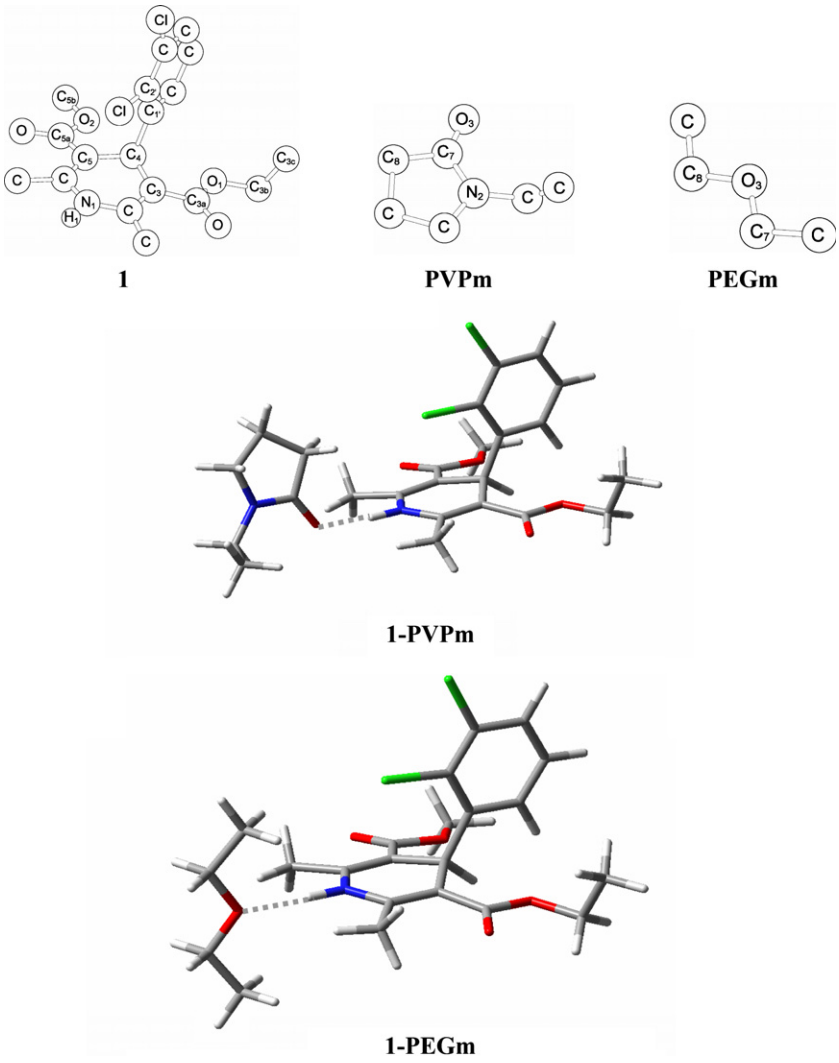

Fig. 6. Optimized structures of felodipine (**1**), PVPm, PEGm, 1-PVPm and 1-PEGm.

In all complexes with PVPm or PEGm a $C_7{=}O_3\cdots H_1{-}N_1$ or a $>O_7\cdots H_1{-}N_1$ hydrogen bond is formed, respectively. The calculated hydrogen bond distance ($N_1\cdots O_3$) is equal to 2.932 and 3.050 Å for the felodipine–PVPm or PEGm complexes, respectively. An interesting structural feature is the elongation of the $N_1{-}H_1$ bond upon formation of the complexes, which is the key factor affecting the predicted infrared properties of the complexes. This elongation is greater in felodipine–PVPm complex (0.014 Å) than in the felodipine–PEGm complex (0.010 Å). All these structural features indicate a stronger hydrogen bonding interaction of felodipine with PVPm than with PEGm. This is further confirmed by the interaction energy values for the two complexes. The BSSE and ZPE corrected interaction energy in 1-PVPm complex was calculated to be equal to −31.8 kJ/mol and is greater than that corresponding to the 1-PEGm complex (−18.8 kJ/mol). An analogous elongation upon formation of the complexes concerns the $C_7{=}O_3$ and $C_{7,8}{=}O_3$ bonds of PVPm and PEG. The hydrogen bonding results in small geometrical rearrangements of felodipine molecule concerning mainly the dihedral angles H–N–C–C. To further examine the binding of felodipine to the terminal hydroxyl groups of the PEG polymer, we have also

Table 2
Selected optimized geometrical parameters[a] of felodipine, **1**, and its hydrogen-bonded complexes 1-PVPm and 1-PEGm[b]

	1	1-PVPm	1-PEGm
$C_2{-}N_1$	1.386	1.382	1.385
$C_6{-}N_1$	1.385	1.382	1.384
$N_1{-}H_1$	1.009	1.023	1.019
$H_1\cdots O_3$		1.914	2.031
$N_1\cdots O_3$		2.932	3.050
$N_1{-}H_1\cdots O_3$		172.8	178.8
$C_7{=}O_3$ (PVPm)		1.238	–
$C_7{-}O_3$ (PEGm)		–	1.451
$C_8{-}O_3$ (PEGm)		–	1.451
$C_4{-}C_3{-}C_{3a}{-}O_3$	174.3	174.7	174.5
$C_4{-}C_5{-}C_{5a}{-}O_5$	7.0	6.3	6.2
$N_1{-}C_4{-}C_{1'}{-}C_{2'}$	0.3	0.4	0.2
$C_{3a}{-}O_1{-}C_{3b}{-}C_{3c}$	−85.5	−85.0	−85.3

[a] In Å and degree.
[b] Numbering scheme as in Fig. 6.

optimized the hydrogen-bonded complex, 1-PEGm, of 1 with the model $CH_3CH_2OCH_2CH_2OH$, with the hydroxylic oxygen acting as hydrogen acceptor in a scheme like $>O\cdots H_1{-}N_1$. The binding energy in this case was calculated to be equal to −33.9 kJ/mol after BSSE and ZPE correction. This value shows a hydrogen bond strength comparable to that in the FELO/PVP system.

3.4. Drug–polymer interactions studied by ^1H NMR spectroscopy

The solubility and dissolution rate of a drug from its solid dispersions would be influenced by the interactions taking place in solution between the drug molecules and the macromolecular chains of the polymer. ^1H NMR spectroscopy was used in order to identify the nature of the interactions between FELO and PVP or PEG that take place in solution. A comparative presentation of the ^1H NMR spectra of pure FELO and of the systems 10/90, 20/80 and 50/50 w/w FELO/PVP and FELO/PEG is shown in Figs. 7 and 8. Several characteristic peaks are observed in the FELO spectrum, but what is of greater interest is the proton that is located on the secondary amino-group and exhibits a resonance at 5.85 ppm (single peak corresponding to one proton). In the solutions prepared from FELO/PVP solid dispersions this peak is

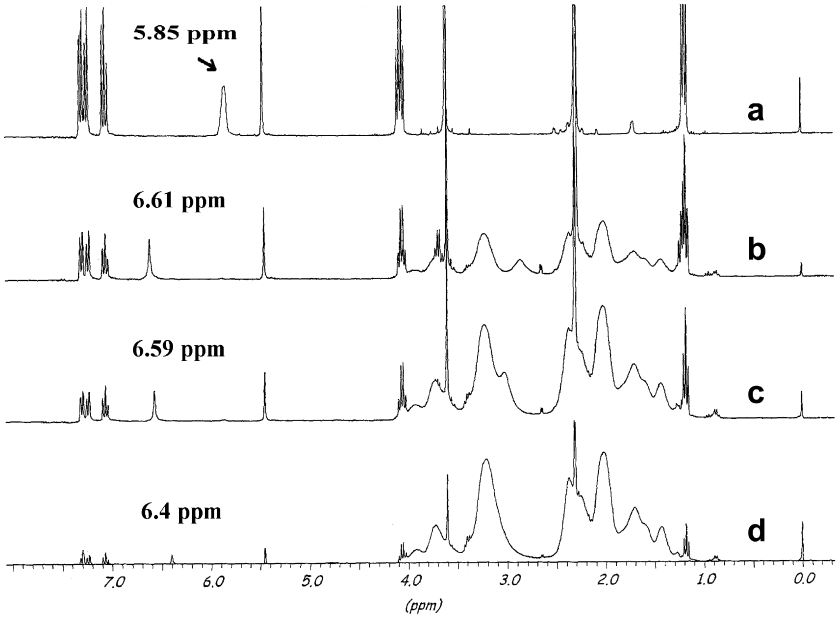

Fig. 7. Proton NMR spectra for (a) pure FELO and FELO/PVP solutions containing (b) 50 wt%, (c) 30 wt% and (d) 10 wt% FELO.

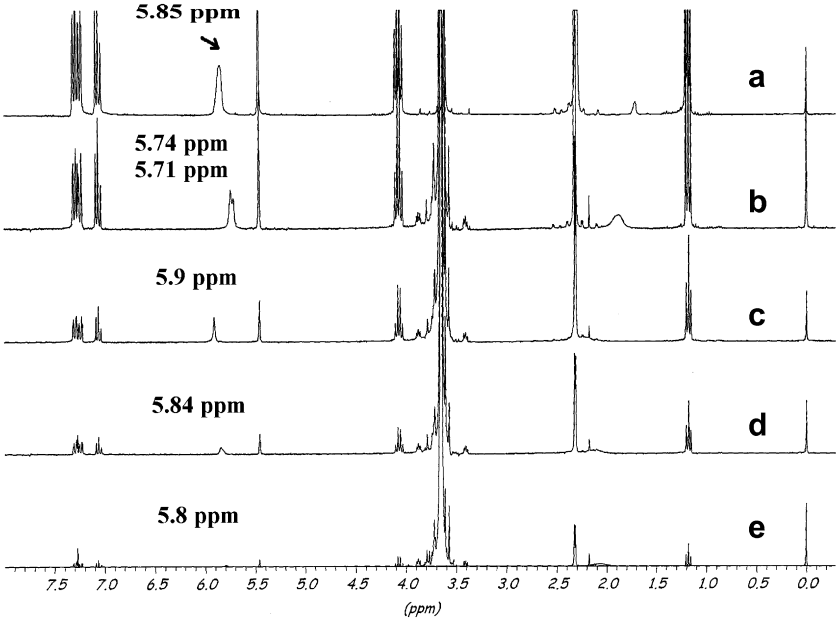

Fig. 8. Proton NMR spectra for (a) pure FELO and FELO/PEG solutions containing (b) 50 wt%, (c) 30 wt% (d) 20 wt% and (e) 10 wt% FELO.

shifted to higher positions with increasing the PVP proportion in the solid dispersion. Thus, in samples containing 10 wt% FELO this peak is recorded at 6.39 ppm while at solutions containing 20 and 50 wt% FELO at 6.57 and 6.62 ppm, respectively. This is an indication that the proton of the secondary amino-group has a lower ability for movements and is more protected. The only case for such protection is the creation of hydrogen bonds with the carbonyl groups of PVP. Additionally, as can be seen in Fig. 7, the position of >NH proton does not further change after 20 wt% of FELO, revealing that the ability of hydrogen bonding formation has been saturated. In the case of FELO/PEG solutions, the position of this proton is almost stable and comparable with that of pure FELO (Fig. 8).

In all solutions, the proton assignment ranged between 5.74 up to 5.9 ppm without exhibiting any clear differences between the different solid dispersions, while in the sample containing 10 wt% FELO the corresponding peak at 5.8 ppm is very weak and hardly detectable. This is evidence that hydrogen bond interactions are very weak in FELO/PEG solutions. So, the ^{1}H NMR data suggest that the intensity of the felodipine–polymer interactions is very low in the FELO/PEG solutions, while hydrogen bonds become stronger in FELO/PVP solutions.

3.5. Particle size evolution during the dissolution of solid dispersions

Before studying the particle size evolution during the dissolution of the solid dispersions, it would be useful to first study the behaviour of the neat polymers (PVP and PEG) during dissolution. In Fig. 9a the volume distribution of particles detected by DLS at different dissolution times of PVP is shown. Very small nanoparticles are formed from the first minutes of dissolution. The volume distribution of these nanoparticles varies with dissolution time. At the initial stages of dissolution (5 min), nanoparticles with medium diameter 8–9 nm exhibiting unimodal size distribution are produced. This type of distribution is also maintained at 10 min, when particles of a medium diameter between 12 and 13 nm were detected. Afterwards, at 20 and 30 min an important differentiation is observed on nanoparticles' formation and the size distribution becomes bimodal, with modes appearing at 8 and 20 nm. The particles' volume with a medium diameter of 8 nm dominates the volume of particles with a diameter of 20 nm. Since the volume of a sphere is equal to $4/3(r)^3$, this distribution implies that the higher number of particles has a medium diameter of 8 nm and only a minimal number of particles have a diameter of 20 nm. A bimodal size distribution is also observed after 50 min dissolution, where most particles have a medium diameter of about 3.5 nm and only a small amount of particles has a diameter of 15 nm. This behaviour shows that, after a certain time interval (30 min), the bigger nanoparticles tend to be reduced into nanoparticles with sizes smaller than 5 nm.

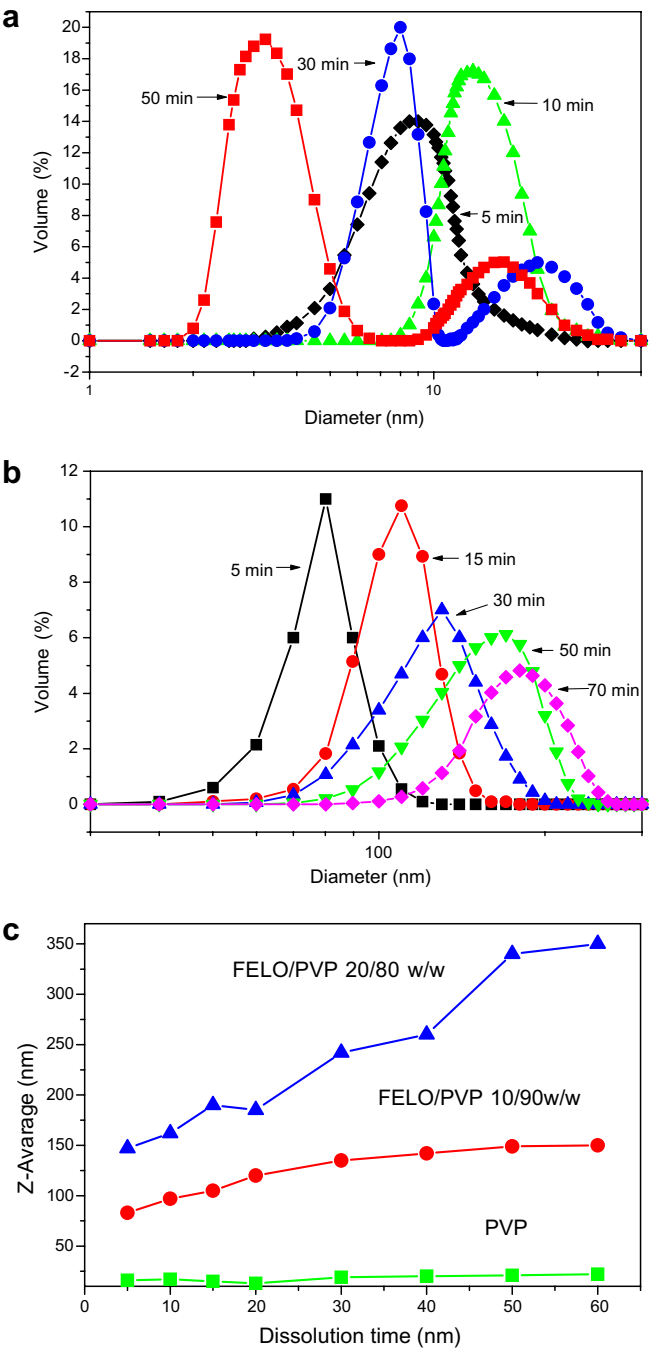

Fig. 9. (a) Particle size distribution (by volume) of PVP particles at different dissolution times. (b) Particle size distribution of FELO/PVP (10/90 w/w) particles at different dissolution times. (c) Average size of particles formed during dissolution of PVP and FELO/PVP solid dispersions.

The small particle sizes observed at 50 min can theoretically be predicted taking into account the configuration of the macromolecular chains in the solution. The behaviour of a flexible polymer chain to transform its conformation from an expanded coil to collapse was verified a long time ago [22]. The free-rotation hypothetical dimension of a polymer chain can be calculated from the number of bonds (n), the bond distance (l) and the bond angle (θ).

$$\langle ro^2f \rangle = nl^2[(1+\cos\theta)/(1-\cos\theta)] \quad (2)$$

For a polymethylene chain like in case of PVP the bond distance is $l = 1.54$ Å and $\theta = 109.5°$. The above relation becomes, then:

$$\langle ro^2f \rangle^{1/2} = 3.08 \times M^{1/2}/Mo^{1/2} \quad (3)$$

where M and Mo the molecular weights of the polymer and the monomer, respectively. For the PVP the following expression can be established [23]:

$$\langle ro^2f \rangle = 290 \times 10^{-11}\ \text{cm}\ M^{1/2} \quad (4)$$

By applying in the above equation $M = 40{,}000$–$50{,}000$, which is the average molecular weight of PVP, the free-rotation hypothetical dimension of PVP is found to range between 5.8 and 6.5 nm (1 cm = 10^7 nm). This theoretical value is very close to that measured with dynamic light scattering process after 50 min of dissolution (Fig. 9a). Examining the above figure it can be seen that the peak range is recorded between 2 and 6 nm. This is evidence that some PVP macromolecules may fold back on themselves into helical conformations reducing their size.

The particles size distribution during dissolution of FELO/PVP solid dispersions is different from that of neat PVP. As can be seen in Fig. 9b, during the dissolution of the solid dispersion containing 10 wt% FELO, bigger particles (than in the case of neat PVP) with a medium diameter of 75 nm are detected at 5 min of dissolution. Their sizes are progressively increased up to 120 nm after 30 min of dissolution. Also, neither a bimodal distribution nor the existence of nanoparticles with very small sizes is observed at high dissolution times, as in neat PVP.

The changes of average particle size distribution for neat PVP as well as for FELO/PVP solid dispersions with dissolution time can be seen in Fig. 9c, where the Z-average is presented. The Z-average can determine with higher precision the sizes of bigger particles formed during dissolution. PVP is rapidly dissolved to particles of sizes up to 20 nm. In the solid dispersion containing 10 wt% FELO, the nanoparticles' size appears to increase progressively with time, but even after 70 min of dissolution the mean particle size is not higher than 200 nm. For the solid dispersion containing 20 wt% FELO, the formed nanoparticles are much bigger than in the case of 10% dispersion. The average particle size in the 20% FELO/PVP dispersions increased with increasing dissolution time, reaching up to 350 nm at 60 min of dissolution.

In the case of PEG, as it can be seen in Fig. 10a, at the very early stages of PEG dissolution (3 min), particles of about 2000 nm are detected, which are decreased rapidly to 500 nm and progressively afterwards to 10–30 nm at 30 min of dissolution time. A similar to the neat PEG trend also appears for the FELO/PEG solid dispersions (Fig. 10a). As the time of dissolution is increased, the particles become progressive smaller. However, the size values recorded at the early (first measurement) and late stages of dissolution (last measurement) depend on the felodipine %

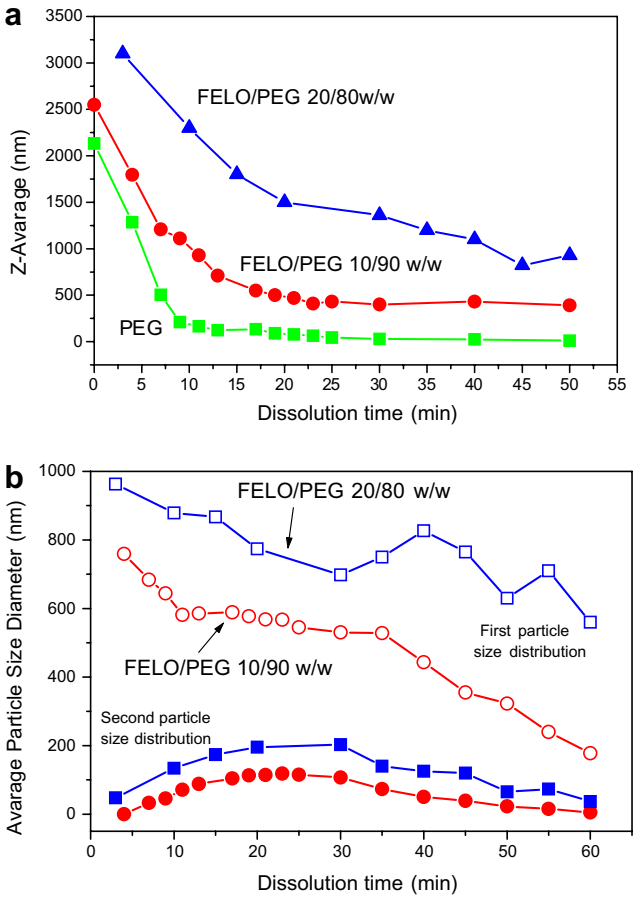

Fig. 10. (a) Average size of particles formed during dissolution of PEG and FELO/PEG solid dispersions and (b) average particle size diameter formed during dissolution of FELO/PEG solid dispersions. In the second diagram, a bimodal distribution is recorded consisting of big and small nanoparticles.

content of the dispersions, both increasing with increasing relodipine content. In all solid dispersions the initially measured sizes are higher than 2000 nm. In the solid dispersions containing 10 and 20 wt% felodipine, the final particle sizes recorded at 60 min of dissolution time were in the range of 500 and 1000 nm, respectively. However, the measurement of the Z-average does not give the real distribution of the particle sizes. Thus, the average particle diameter was also measured which can distinguish the existence of different particle sizes. As can be seen in Fig. 10b a bimodal distribution of the particle sizes is recorded for the measured solid dispersions. Particles with bigger sizes as well as particles with nanosizes are detected. This bimodal distribution was also evaluated with SEM.

As it can be seen from SEM micrographs of particles collected at different times of dissolution of FELO/PEG 10/90 w/w solid dispersion, after 5 min of dissolution except for the particles with sizes 1–5 μm there are particles in the range of 1500–2000 nm (Fig. 11a). Furthermore, nanoparticles in the range of 100–200 nm can also be observed as already recorded with the Malvern instrument (Fig. 10b). After 15 min of dissolution, the size of the

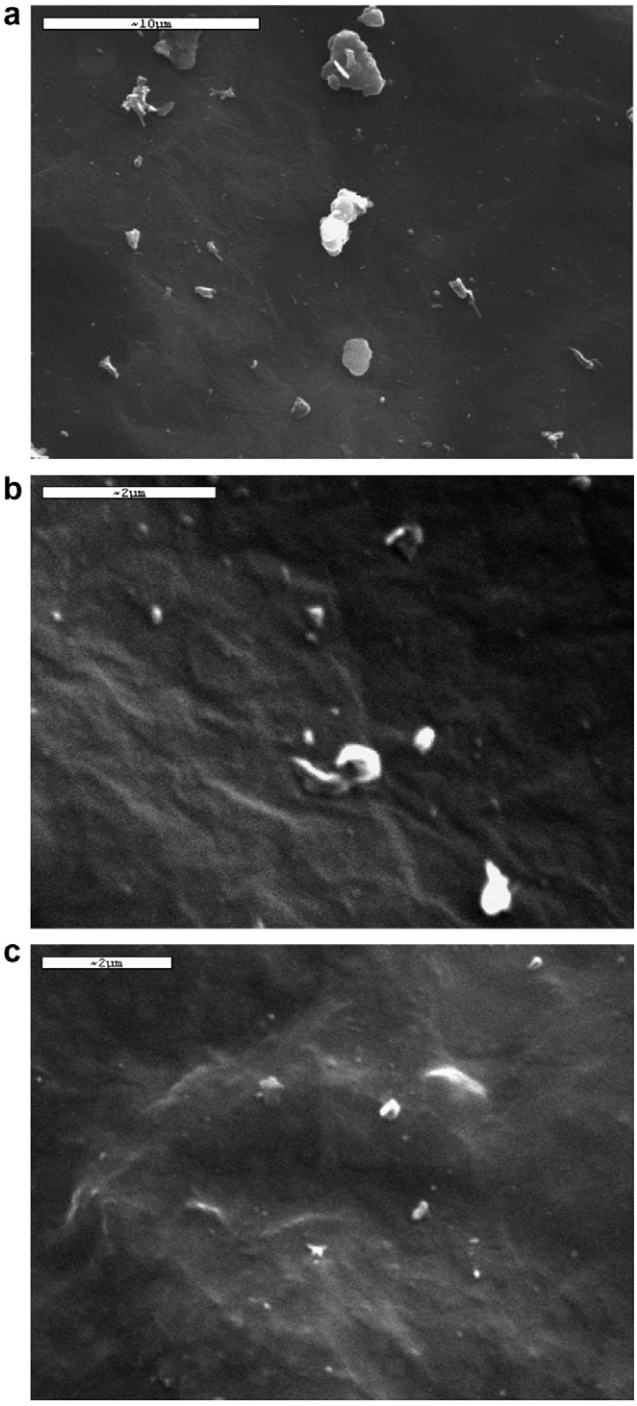

Fig. 11. SEM micrographs of FELO/PEG 10/90 w/w solid dispersion during dissolution for (a) 5 min, (b) 15 min and (c) 30 min.

particles is reduced, and particles with diameters higher than 1000 nm could not be seen. After 30 min of dissolution, only particles smaller than 300–400 nm could be observed. In both micrographs (Figs. 11b and c), very small nanoparticles with sizes lower than 50–60 nm can be seen. These findings are in line with the bimodal distribution of particle size observed during dissolution of FELO/PEG dispersions with the DLS technique (Fig. 10b).

4. Discussion

FELO exhibits high permeability through biological membranes, but its absorption after oral administration is limited by its low dissolution rate, due to its very low aqueous solubility (lower than 0.5 mg/lt). In order to increase the dissolution rate of FELO, several attempts have been made in the past. Since FELO is a crystalline compound, most of these attempts deal with preparation of the glassy state of the drug [24–27]. From our previous studies, it was found that enhancement of FELO dissolution can be achieved by employing hydrophilic matrices, such as modified celluloses [28] and, especially, PVP [13,29]. In this work, the mechanism of FELO release from solid dispersions in PVP and PEG was investigated.

Based on the FT-IR spectra (Fig. 5), FELO interacts through H-bonding with both polymers, albeit this interaction appears to be stronger in the case of PVP. The latter is supported by the results of theoretical calculations based on quantum mechanics and the density functional theory [14,15] for the optimization of the complexes formed between FELO and polymer model structures (Fig. 6). The elongation of the N_1—H_1 bond upon formation of the complex was calculated to be greater in the FELO–PVP complex than in the FELO–PEG complex, and the same was found for the interaction energy values for the two complexes. All these data indicate the existence of a stronger interaction between FELO and PVP than between FELO and PEG. Further confirmation of the latter was provided by a detailed vibrational analysis of the complexes: the red shift of the N—H bond stretching in FELO molecule due to H-bonding was higher in the case of FELO–PVP complex than in the case of FELO–PEG (in line with the experimental FT-IR data), indicating a stronger H-bond in the case of FELO–PVP [30].

Probably due to the stronger interactions at the molecular level of FELO with PVP than with PEG, FELO is dispersed as amorphous nanoparticles in the case that PVP is used as the drug carrier (as the XRD and TEM data for FELO/PVP dispersions, Figs. 2 and 3, indicate) and in the form of crystalline microparticles in the PEG carrier (as the XRD and SEM data for FELO/PEG dispersions, Figs. 2 and 4, indicate). Based on these characteristics of the two types of solid dispersions, a higher dissolution rate of FELO from the dispersions in PVP was anticipated. However, the release rate of FELO was similar from both types of dispersion at low FELO contents (10% and 20% drug w/w), and only at high drug loading (50% drug w/w) the rate of release was lower from the dispersion in PEG than in PVP (Fig. 1). These results suggest that the rate of FELO release from the two dispersions is significantly influenced, at least at high drug contents, from another factor besides the rate of drug particle dissolution (i.e. the rate of drug molecules' detachment from the drug particles, which will be much faster in the case of FELO/PVP dispersions due to the amorphous drug state and the small size of drug particles). Drug

release involves two successive processes: the detachment of the drug molecule from the drug particles and the diffusion of the solvated molecule through the diffusion layer. Experimental evidence that drug diffusion contributes to the overall drug release profile provides the fact that, at dissolution times that drug has completely been released (100% release), particles of the solid dispersion could still be detected in the dissolution medium. For example at 30 min, when FELO release from the 10/90 FELO/PVP and FELO/PEG dispersions was complete (Fig. 1), particles of the dispersions were found to exist in the dissolution medium (particles detected by DLS and/or observed by SEM, Figs. 9–11).

The diffusion layer in the solid dispersions with high polymer content would mainly consist of the more rapidly dissolving and more abundant component, i.e. PVP and PEG in the FELO/PVP and FELO/PEG dispersions, respectively. In our case, PVP has a much higher molecular weight than PEG and will probably form a much more viscous diffusion layer than PEG (perhaps of a gel consistency since PVP swells in water forming hydrogels). It is, then, reasonable to assume that the diffusion of FELO through the diffusion layer would be slower in the case of the FELO/PVP dispersions than in the case of FELO/PEG dispersions. To the slower FELO diffusion through the PVP layer compared to the PEG layer could also contribute the stronger interactions in solution of FELO molecules with PVP molecules than with PEG molecules, as revealed by ^{1}H NMR (Figs. 7 and 8), which would retard the movement of drug molecules towards the bulk of the dissolution medium in the case of PVP carrier. It is probably the slow diffusion of FELO molecules through the PVP diffusion layer that slows down the overall rate of FELO release from the FELO/PVP dispersions with low drug content, rendering it similar to that observed with the FELO/PEG dispersions of the same low drug content (Fig. 1).

At high drug content (50% FELO), the relatively low polymer amount around the drug particles probably dissolves rapidly, exposing the drug particles to the dissolution medium. Then, dissolution of the drug particles (and not drug diffusion) should dominate drug release and, due to the characteristics of the drug particles in the two types of dispersion studied (amorphous nanoparticles in PVP as opposed to crystal microparticles in PEG), the release rate should be higher in the case of FELO/PVP dispersions than in the case of FELO/PEG dispersions. Indeed, the rate of FELO release was higher from the FELO/PVP dispersion with 50% drug content than from the FELO/PEG dispersion with the same drug content (Fig. 1). That FELO release from the solid dispersions studied here is diffusion-dominated at low drug proportions and dissolution-dominated at high drug proportions is supported by the analysis of release kinetics according to a release function which includes both diffusion and dissolution components Eq. (1). The two-term equation has been used to analyze drug release from hydrophilic, swellable/soluble polymers, such as the ones used here, providing information on the relative contribution of drug diffusion and polymer dissolution in drug release [31]. In our case, it is probably the dissolution of the drug, and not the polymer dissolution, that governs drug release at high drug proportions in the matrix, due to the very low aqueous solubility of felodipine. Support for this consideration provides the decrease of drug release rate with decreasing polymer proportion in the solid dispersions (i.e. increasing drug proportion, Fig. 1). If polymer dissolution governed release, an increase of release rate with decreasing polymer proportion should have been observed. The results of the release data analysis (Table 1) suggest that about 80% of drug content is released through diffusion in the case of FELO/PVP 10/90 dispersion as opposed to only about 7% in the case of FELO/PVP 50/50 dispersion (respective values for FELO/PEG dispersions 73% and 7%). The kinetics analysis also indicates that the relative contribution of dissolution (compared to diffusion) to drug release was found to be higher in the FELO/PEG dispersions than in FELO/PVP dispersions (especially at low drug proportions), a reasonable outcome if one considers that the low molecular weight PEG probably forms a less dense and thick diffusion layer around drug particles than the high molecular weight PVP and, therefore, drug diffusion exerts a less significant influence on drug release than particle dissolution in the case of PEG.

A decrease in FELO release rate with increasing FELO content was observed with both types of solid dispersions (Fig. 1). This appears to be invariably the case with the solid dispersions of drugs and, in our case, may be attributed to the increased size of FELO particles with increasing FELO content of the dispersions (Figs. 3 and 4). The observed increase of the size of the (relatively small) particles which are formed early in the dissolution process with increasing drug content of the dispersion (Figs. 9 and 10) may also contribute to the observed decrease of drug release rate with increasing drug content of the dispersion.

The results of particle size measurements during dissolution of the solid dispersions indicate that, after introducing them in the dissolution medium, the large initial particles of both types of solid dispersions (FELO/PVP and FELO/PEG) containing relatively low amounts of drug are very rapidly decreased to smaller particles, including nanoparticles (DLS and SEM data, Figs. 9–11). During this rapid size reduction, an extreme increase of the surface exposed to the dissolution medium occurs, leading to the impressive enhancement of FELO dissolution rate observed with the dispersions of relatively low drug content (10% and 20% drug w/w). For example, there was approx. 40% drug release within the first 5 min of dissolution time for both FELO/PVP and FELO/PEG 10/90 w/w dispersions, as opposed to only 0.5% of drug dissolution at the same period (5 min) for pure FELO (Fig. 1). What causes this rapid decrease of the size of the solid dispersions containing low amount of drug once within the dissolution medium is not clear. One could speculate that the presence of the sodium

docusate surfactant in the structure of the solid dispersion particles and the presence of polysorbate 20 in the dissolution medium may accelerate particle dissolution through their wetting and solubilization functions. That the drug is found in fine subdivision in the dispersions with low drug contents (Figs. 3 and 4) may also enhance particle dissolution and contribute to the rapid decrease of the particle size. However, the phenomenon needs investigation.

In the case of the solid dispersions containing high amounts of drug (FELO/PVP and FELO/PEG 50/50 w/w), no such rapid reduction of the size of the solid dispersion particles takes place during dissolution (data not shown). The dominant mechanism of drug release is the dissolution of the drug particles, and as these are relatively coarse in this case (compared to the dispersions with low drug content, Figs. 3 and 4), a relatively slow release profile is obtained (Fig. 1). Another cause, probably complementary to the increased size of drug particles, for the relatively low rate of drug release from the 50/50 w/w dispersions might be the inadequate wetting of the solid dispersion particles, due to the presence of high amount of hydrophobic drug in their structure. Studies on wetting of heterogeneous surfaces have indicated that the hydrophobic portion of the surface ultimately determines the wettability of the specimen [32]. Nevertheless, FELO release from the 50/50 solid dispersions still is much more rapid than the dissolution of pure FELO (Fig. 1), presumably because the initial size of drug particles is much smaller in the case of the solid dispersions.

5. Conclusions

The interactions at the molecular level of FELO with the polymer carrier (PVP and PEG) appeared to control the physical state (amorphous or crystalline) and the particle size of FELO in the solid dispersions of FELO in PVP or PEG. When these interactions are relatively strong, as in the case of FELO/PVP dispersions, the drug forms amorphous particles in the nano-range of sizes. If they are relatively weak, as in the case of FELO/PEG solid dispersions, the drug is dispersed as crystals having sizes in the micro-range. The size of drug particles in the dispersion is also influenced by drug proportion, with an increase in drug content of the dispersion resulting in increased drug particle size. The particle size of drug, the proportion of drug in the dispersion and the properties of the polymer (molecular weight) appeared to determine the mechanism of drug release from particulate solid dispersions of drug in PVP or PEG, which was drug diffusion (through the polymer layer)-controlled at low drug contents and drug dissolution-controlled at high drug contents. The large initial particles of both types of solid dispersions (FELO/PVP and FELO/PEG) with low drug content are very rapidly decreased to smaller particles (including nanoparticles) during dissolution, leading to an impressive enhancement of FELO release rate from these dispersions.

References

[1] A.T.M. Serajuddin, Solid dispersions of poorly-water soluble drugs: Early promises, subsequent problems and recent breakthroughs, J. Pharm. Sci. 88 (1999) 1058–1066.
[2] W.L. Chiou, S. Riegelman, Pharmaceutical applications of solid dispersions, J. Pharm. Sci. 60 (1971) 1281–1302.
[3] D.Q.M. Craig, The mechanisms of drug release from solid dispersions in water-soluble polymers, Int. J. Pharm. 231 (2002) 131–144.
[4] H. Friedrich, B. Fussnegger, K. Kolter, R. Bodmeier, Dissolution rate improvement of poorly water soluble drugs obtained by absorbing solutions of drugs in hydrophilic solvents onto high surface area carriers, Eur. J. Pharm. Biopharm. 62 (2006) 171–176.
[5] E. Sjokvist-Saers, D.Q.M. Craig, An investigation into the mechanisms of dissolution of alkyl *p*-aminobenzoates from polyethylene glycol solid dispersions, Int. J. Pharm. 83 (1992) 211–219.
[6] D. Hörter, J.B. Dressman, Influence of physicochemical properties on dissolution of drugs in the gastrointestinal tract, Adv. Drug Deliv. Rev. 56 (2001) 75–87.
[7] E. Sjokvist, C. Nystrom, Physicochemical aspects of drug release. VI. Drug dissolution rate from solid particulate dispersions and the importance of carrier and drug particle properties, Int. J. Pharm. 47 (1988) 51–66.
[8] O.I. Corrigan, Mechanisms of dissolution of fast release solid dispersions, Drud. Dev. Ind. Pharm. 11 (1985) 697–724.
[9] D.Q.M. Craig, J.M. Newton, The dissolution of nortryptiline HCl from polyethylene glycol solid dispersions, Int. J. Pharm. 78 (1992) 175–182.
[10] S. Bogdanova, I. Pajeva, P. Nikolova, I. Tsakovska, B. Müller, Interactions of poly(vinylpyrrolidone) with ibuprofen and naproxen experimental and modelling studies, Pharm. Res. 22 (2005) 806–815.
[11] K. Khougaz, S.D. Clas, Crystallization inhibition in solid dispersions of MK-0591 and poly(vinyl pyrrolidone) polymers, J. Pharm. Sci. 89 (2000) 1325–1334.
[12] E. Karavas, G. Ktistis, A. Xenakis, E. Georgarakis, Effect of hydrogen bonding interactions on the release mechanism of felodipine from nanodispersions with polyvinylpyrrolidone, Eur. J. Pharm. Biopharm. 63 (2006) 103–114.
[13] B. Abrahamsson, D. Johansson, A. Torstensson, K. Wingstrand, Evaluation of solubilizers in the drug release of hydrophilic matrix extended-release tablets of felodipine, Pharm. Res. 11 (1994) 1093–1097.
[14] M.J. Frisch, G.W. Trucks, H.B. Schlegel, G.E. Scuseria, et al., Gaussian 98, Revision A.7, Gaussian Inc., Pittsburgh PA, 1998.
[15] M. Rosenberg, A. Loewenschuss, Y. Marcus, An empirical correlation between stretching vibration red shift and hydrogen bond length, Phys. Chem. Chem. Phys. 2 (2000) 2699, and references therein.
[16] R.S. Harland, A. Gazzaniga, E.M. Sangali, P. Colombo, N.A. Peppas, Drug/polymer matrix swelling and dissolution, Pharm. Res. 5 (1988) 488–494.
[17] E. Karavas, E. Georgarakis, D. Bikiaris, Felodipine nanodispersions as active core for predictable pulsatile chronotherapeutics using PVP/HPMC blends as coating layer, Int. J. Pharm. 313 (2006) 189–197.
[18] D. Bikiaris, G.Z. Papageorgiou, A. Stergiou, E. Pavlidou, E. Karavas, F. Kanaze, M. Georgarakis, Physicochemical studies on solid dispersions of poorly-water soluble drugs. Evaluation of capabilities and limitations of thermal analysis, Thermochem. Acta 439 (2005) 58–67.
[19] (a) A.M. Kaushal, P. Gupta, A.K. Bansal, Amorphous drug delivery systems: molecular aspects, design and performance, Crit. Rev. Ther. Drug Carrier Syst. 21 (2004) 133–193;
(b) Piyush Gupta, A.K. Bansal, Devitrification of Amorphous Celecoxib, AAPS Pharm. Sci. Tech. 6 (2005) E223–E230.
[20] T. Chiavassa, P. Roubin, L. Pizzala, P. Verlagne, A. Allouche, F. Marinelli, Experimental and theoretical studies of malonaldehyde vibrational analysis of a strong intermolecular hydrogen bonded compound, J. Phys. Chem. 96 (1992) 10659–10665.

[21] H. Rostkowska, M.J. Nowak, L. Lapinski, L. Adamowicz, IR spectral and theoretical characterization of intermolecular hydrogen bonds closing fivemembered rings, Phys. Chem. Chem. Phys. 3 (2001) 3012–3017.
[22] W.H. Stockmayer, Estimation of unperturbed dimensions from intrinsic viscosities, Macromol. Chem. 35 (1960) 54–58.
[23] R. Meza, L. Gargallo, Unperturbed dimensions of polyvinylpyrrolidone in pure solvents ad in binary mixtures, Eur. Polym. J. 13 (1977) 235–239.
[24] D.H. Won, M.S. Kim, S. Lee, J.S. Park, S.J. Hwang, Improved physicochemical characteristics of Felodipine solid dispersion particles by supercritical anti-solvent precipitation process, Int. J. Pharm. 301 (2005) 199–208.
[25] J. Kerč, S. Srčič, Ž. Knez, P. Senčar-Božič, Micronization of drugs using supercritical carbon dioxide, Int. J. Pharm. 182 (1999) 33–39.
[26] B.K. Kim, S.J. Hwang, J.B. Park, H.J. Park, Characteristics of Felodipine-located poly(ε-caprolactone) microparticles, J. Microencapsul. 22 (2005) 193–203.
[27] E. Karavas, E. Georgarakis, D. Bikiaris, T. Thomas, V. Katsos, A. Xenakis, Hydrophilic matrices as carriers in felodipine solid dispersion systems, Prog. Colloid Polym. Sci. 118 (2001) 149–152.
[28] E. Karavas, G. Ktistis, A. Xenakis, E. Georgarakis, Miscibility behaviour and formation mechanism of stabilized felodipine-polivinylpyrrolidone amorphous nanodispersions, Drug Dev. Ind. Pharm. 31 (2006) 473–489.
[29] E. Karavas, E. Georgarakis, D. Bikiaris, Application of PVP/HPMC miscible blends with enhanced mucoadhesive properties for adjusting drug release in predictable pulsatile chronotherapeutics, Eur. J. Pharm. Biopharm. 64 (2006) 115–126.
[30] P. Gupta, R. Thilagavathi, A.K. Chakraborti, A.K. Bansal, Role of molecular interactions in stability of celecoxib-PVP amorphous systems, Mol. Pharm. 2 (2005) 384–391.
[31] J. Sujja-arreevath, D.L. Munday, P.J. Cox, K.A. Khan, Relationship between swelling, erosion and drug release in hydrophilic natural gum mini-matrix formulations, Eur. J. Pharm. Sci. 6 (1998) 207–217.
[32] G. Buckton, J.M. Newton, Assessment of the wettability of powders by use of compressed powder discs, Powder Technol. 46 (1986) 201–208.